Performance of Nonstructural Components in a Controlled Rocking Steel Braced Frame Structure

Nathan Buccella[1], Lydell Wiebe[2], Dimitrios Konstantinidis[3], Taylor Steele[4]

[1] M.A.Sc. Student, Department of Civil Engineering, McMaster University - Hamilton, ON, Canada.
[2] Associate Professor, Department of Civil Engineering, McMaster University - Hamilton, ON, Canada.
[2] Assistant Professor, Department of Civil and Environmental Engineering, UC Berkeley - Berkeley, CA, USA.
[4] Ph.D. Candidate, Department of Civil Engineering, McMaster University - Hamilton, ON, Canada.

ABSTRACT

Controlled rocking steel braced frames (CRSBFs) have shown promising structural performance during earthquakes, but in order for this seismic force resisting system to be used as a high-performance design alternative, the performance of nonstructural components in the system should not be compromised. Recent studies have shown mixed results in assessing the performance of attached nonstructural components in CRSBFs. In this study, the performance of attached nonstructural components in four three-storey CRSBFs with varying hysteretic design parameters (energy dissipation, prestressing ratio and frame stiffness) is evaluated numerically. The CRSBFs were designed to reach similar median peak drifts, suggesting similar performance of drift-sensitive components and allowing for a comparison of demands on acceleration-sensitive components that is not influenced by drift performance. The results show that the magnitude and location of floor spectra peaks in CRSBFs depend primarily on the stiffness of the frame, rather than the energy dissipation and prestressing provided. Although the magnitudes of the floor spectra peaks can be reduced by designing CRSBFs of equivalent frame stiffness with more energy dissipation, the reduction is minor for the cases considered.

Keywords: Controlled Rocking, Nonstructural Components, High-Performance System, Floor Spectra, Self-Centering, Operational and Functional Components

INTRODUCTION

In the push for seismically resilient structures, controlled rocking steel braced frames (CRSBFs) have been developed as an economical solution to meet seismic drift demands while reducing structural damage and residual drifts. CRSBFs are intentionally allowed to uplift from the foundation, and this uplifting action acts as the force-limiting mechanism for the system, rather than member yielding. Self-weight and, in most cases, prestressed tendons anchoring the frame to the foundation provide a restoring force during rocking. A variety of different energy dissipating devices engaged by uplift can also be provided, typically at the column bases. The result is a system where the members of the frame are capacity protected, self-centering ensures minimal residual drifts, and damaged energy dissipating fuses can be replaced. Figure 1 displays the flag-shaped hysteresis typical of controlled rocking systems. The initial stiffness is provided by the braced frame before it uplifts. Once the frame uplifts, the second stiffness is provided by the axial stiffness of the prestressed tendon and the energy dissipation devices, which also provide the flag-shaped area of the hysteresis. As the frame self-centers, coming back into contact with the foundation, the system again experiences the elastic stiffness of the frame while also passing through its initial rested position before it uplifts in the opposite direction.
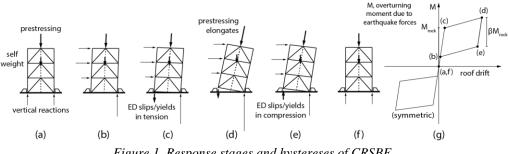

Figure 1. Response stages and hystereses of CRSBF.

Extensive research has been conducted to show that CRSBFs can be successfully designed to meet drift demands at and above the design level while also minimizing residual drifts [1-3]. Although CRSBFs have shown promising structural performance, in order for the building to be considered seismically resilient, the satisfactory performance of nonstructural components is also important. It has been shown that upwards of 85% of a building's value is typically in the nonstructural components [4]. One concern for nonstructural component performance in CRSBFs is whether the higher mode effects, shown to increase frame member forces [1-3,5], will also translate to heightened acceleration spectra at the floor levels. Also of concern is how the abrupt changes in system stiffness will affect floor acceleration spectra, particularly when the CRSBF changes from the low system stiffness experienced during rocking to the high stiffness experienced when the frame comes back in contact with the foundation [6]. Dyanati et al. [7] compared the seismic performance of a self-centering concentrically braced frame to a conventional concentrically braced frame and found that although the self-centering frame had better structural performance, the demands on acceleration-sensitive nonstructural components were larger. To improve the performance of acceleration-sensitive nonstructural components in CRSBFs by mitigating large magnitudes in floor spectra, Pollino [8] suggested increasing frame rigidity or allowing for inelastic deformation of the CRSBF brace members.

Due to the nature of a CRSBF's rocking mechanism, the system can be designed with many different combinations of energy dissipation, prestressing, frame stiffness, and post-uplift stiffness, as well as a variety of response modification factors. For this reason, this research seeks to analyze the performance of attached nonstructural components in varying CRSBF designs which, despite having different hysteretic design parameters, have all been designed to meet the same seismic drift performance. In this regard, four variations of a three-storey CRSBF structure are designed to resist the seismic forces for a design basis earthquake (DBE) on a site in the western United States, based on the seismic hazard in ASCE 7-16 [9]. The base rocking joint is designed based on the methodology set out by Wiebe and Christopoulos [10], in combination with the regression equations developed by Zhang et al. [11] as a preliminary estimate of the expected seismic drifts. The CRSBF frame members are capacity designed based on the dynamic procedure proposed by Steele and Wiebe [12]. Each CRSBF is then modelled in OpenSees [13] and time-history analyses are performed for a suite of 44 ground motions. After iterating each design to reach the target seismic drift of 1.5% based on time-history analysis, the performance of attached acceleration-sensitive components is assessed by means of floor spectra.

DESIGN OF CONTROLLED ROCKING STEEL BRACED FRAMES

The designed building is a three-storey structure located in the western United States. The mapped MCE_R spectral response acceleration parameter values at short periods and at 1 second are $S_S = 1.5$ g and $S_1 = 0.6$ g, respectively. The structure is located on a Class D site, defined in ASCE 7-16 [9] as a stiff soil with 183 m/s $\leq v_s \leq$ 366 m/s. The short-period site coefficient is $F_a = 1$, and the long-period site coefficient is $F_v = 1.7$. The resulting DBE spectrum is shown in Figure 2 (a). The layout of the structure's gravity system is shown in Figure 2 (b). The building is a 6 by 4 bay structure with identical bay widths of 9.144 m, and the height of each storey is 4.572 m. The seismic weight of the floor and roof levels is 10 090 kN and 6440 kN, respectively. Based on the magnitudes of the design base shears, it was determined that two CRSBFs per direction would be acceptable in resisting the seismic forces for the three-storey structures. The target peak seismic drift for the CRSBF designs was 1.5% and was chosen based on the allowable storey drift per ASCE 7-16 for a structure in the "all other structures" category of risk category III. Each CRSBF was designed with chevron bracing, with the prestressing located at the centre of the frame, and with friction energy dissipation devices located at the base of each column. Since the CRSBF must fit inside the gravity framing, the width of the CRSBF was assumed to be 80% of the bay width. The CRSBFs designed in this study do not carry the gravity loads of the floor and roof diaphragms.
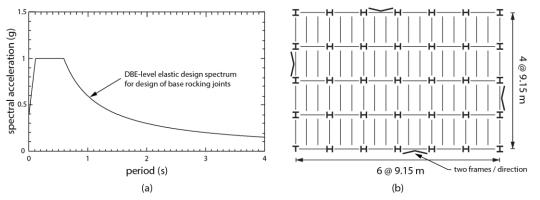

Figure 2. Designed structure: (a) DBE spectrum, (b) structural layout.

Typically, the design of each CRSBF is split into two distinct processes [10, 14]. First, the rocking joint is designed so that the resulting moment needed to cause uplift is larger than the overturning moment caused by the reduced seismic forces defined

by the code. The prestressing strain at the maximum design drift must also be checked to ensure the prestressing remains elastic. The second step is capacity designing the frame member sections. Since the plastic mechanism for a CRSBF is the rocking motion, the frame members are designed to remain elastic to maintain the initial stiffness of the system and to ensure that any repair to the system following an earthquake does not involve replacing the frame members. Both design processes are discussed in detail below.

In this study, a special design requirement was also enforced. The code prescribes a maximum allowable seismic drift, in this case 1.5%, and allows for the peak drifts to be anywhere below this value. In this paper, after each CRSBF was designed and time-history analyses were completed, only CRSBFs whose median peak seismic drifts were within 10% of the target seismic drift of 1.5% were deemed acceptable designs. The purpose of this design stipulation was to ensure that the generated floor spectra could be compared for CRSBF systems that impose similar drift demands on drift-sensitive components.

CRSBF Design Part I: Base Rocking Joint Design

In order to design the rocking joint of the CRSBF, the methodology set out by Wiebe and Christopoulos [10] was used with one modification in estimating the seismic drifts: the regression equation developed by Zhang et al. [11] for initial stiffness proportional damping was applied instead of using the design charts provided by Wiebe and Christopoulos [10].

The first step in the rocking joint design process involves choosing the response modification factor, R, the energy dissipation parameter, β (twice the ratio of the moment resistance provided by energy dissipation to the rocking moment, as shown in Figure 1 (g)), and estimating the fundamental period, T_1. These values are required to estimate the drifts of the CRSBF using the regression equation developed by Zhang et al. [11]. Although the value of β was kept constant for each design, the values of R and T_1 changed through each design iteration as the rocking joint and frame members were redesigned.

The properties of the structure were then idealized into an SDOF system. After an effective mass (m_{eff}) and effective height (H_{eff}) of the frame were calculated, the minimum base rocking moment ($M_{b,rock}$) necessary to resist the code design forces was calculated as:

$$M_{b,rock} \geq S_{a,DBE}(T_1)m_{eff}H_{eff}/R \tag{1}$$

where $S_{a,DBE}(T_1)$ is the spectral acceleration at the fundamental period based on the design spectrum. It should be noted that after the preliminary CRSBF design was completed, the code prescribed lateral force distribution was used to determine $M_{b,rock}$ for the subsequent design iterations.

The next step was designing $M_{b,rock}$ to resist the overturning moment shown in Eq. (1). $M_{b,rock}$ is equal to the sum of the moments resisting overturning:

$$M_{b,rock} = M_w + M_{ED} + M_{PT} \tag{2}$$

where M_W is the moment resistance provided by the self-weight of the CRSBF (since the frame does not carry the other gravity loads of the structure), M_{ED} is the moment resistance provided by the energy dissipation device, and M_{PT} is the moment resistance provided by the prestressing. M_{ED} was calculated using the chosen value of β, leaving M_{PT} to be calculated as the remaining moment needed to exceed the minimum base rocking moment determined by the code spectral acceleration. Once these three moments were calculated, the force provided by the friction energy dissipation device, the prestressing cross-sectional area, and the initial prestress were calculated using the moment arms of each to the rocking toe. Finally, based on the designed prestress ratio, the prestressing was checked to ensure it would not yield at the design drift. If this check was satisfied, the rocking joint design was considered complete and the frame members of the CRSBF were capacity designed, as described in the following section. After the frame members were capacity designed, the true natural period of the CRSBF was calculated, and the seismic drifts were checked using the regression equation [11]. If the drifts did not meet the target design drift, the rocking joint design was iterated by increasing $M_{b,rock}$.

CRSBF Design Part II: Frame Member Capacity Design

Once the base rocking joint was designed, the frame members of the CRSBF were capacity designed to ensure they remained elastic during the earthquake. Steele and Wiebe [12] proposed both an equivalent static and dynamic capacity design procedure. The present study used the dynamic procedure to calculate the design forces for the frame members. This method uses an elastic model of the frame as it rocks about one of its toes, and combines the force effects experienced by the frame members in the primary rocking mode with the force effects caused by the frame vibrating in higher modes as it rocks about the toe.

An example elastic model for the dynamic procedure is shown in Figure 3 (a). The estimation of frame member forces is split into two steps. The forces developed in the frame members due to the CRSBF rocking to its ultimate base rotation, based on the rocking joint design, are calculated by applying the lateral force distribution calculated using ASCE 7-16 [9] amplified by

the overstrength of the rocking joint design, Ω. This is done to emulate the frame rocking to its ultimate displacement, which also brings the prestressing to the expected tensile force experienced at the ultimate base rotation. The calculated member forces based on the ultimate rocking displacement are then combined with an estimation of the force contributions from the frame vibrating in higher modes. This is done through a modal analysis that only includes the contributions from the modes higher than the fundamental mode of the rocking CRSBF. To ensure the frame members remain elastic, the modal analysis for higher modes was conducted using the MCE spectral accelerations when the rocking joint has been designed for the DBE case. The MCE spectrum truncated to consider only modes above the fundamental rocking mode is shown in Figure 3 (b).
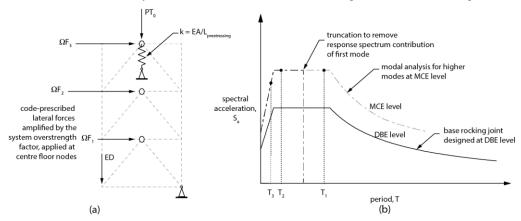

Figure 3. Capacity design dynamic procedure: (a) elastic frame model, (b) DBE spectrum and truncated MCE spectrum.

CRSBF Design Part III: Iteration Based on Time-History Analysis Results

To facilitate a fair comparison of floor accelerations and spectra when the structure achieves the target drift of 1.5%, the design of the rocking joint was iterated based on the results of median peak drift from the time-history analysis of each CRSBF. During design iteration, the designer can reduce the peak drifts by increasing the base rocking moment (i.e. reducing *R*), increasing the energy dissipation parameter *β,* or altering the fundamental period of the system by redesigning the frame members. Since frame overdesign is expected to be more expensive than altering the prestressing or energy dissipation force, the rocking joint was redesigned first by adjusting *R* without changing *β,* and then the frame member capacity design was carried out using the new rocking joint design, rather than immediately stiffening the frame to control drifts. The base rocking joint was adjusted to bring the median peak drifts to within 10% of the 1.5% target drift. In some cases, the capacity design with the iterated rocking joint changed the design of the frame members, thereby also changing the fundamental period of the CRSBF. The ground motions were then rescaled to the new fundamental period before commencing with the new time-history analysis. Table 1 displays the final CRSBF designs and selected results from the time-history analyses. The variable *η* represents the ratio of initial prestress to the ultimate strength of the prestressing tendons. The PT force and ED force represent the initial prestress force of the prestressing and plastic force exerted by the friction energy dissipation device, respectively.

Table 1. Final CRSBF designs.

β (%)	η (%)	PT Force (kN)	ED Force (kN)	R	T_1 (s)	T_2 (s)	T_3 (s)	Median Peak Drift (%)	Columns Buckled (# of records)	Braces Buckled (# of records)
25	20	3017	229	10.00	0.420	0.141	0.102	1.45	1/44	1/44
25	40	3932	293	7.80	0.476	0.160	0.118	1.35	0/44	7/44
90	20	1612	720	11.43	0.513	0.174	0.129	1.41	1/44	6/44
90	40	1852	802	10.26	0.554	0.189	0.144	1.47	3/44	6/44

GROUND MOTION SELECTION AND SCALING

The far-field record set selected in FEMA P695 [15] was used for the time-history analysis. This record set consists of 44 ground motions from 22 different earthquakes (two components each) that have been selected based on the requirements set out in FEMA P695. The ground motions selected are from large magnitude (magnitude 6.5 or greater) strike-slip or reverse (thrust) earthquakes. No ground motion has a peak ground acceleration or peak ground velocity of less than 0.2 g and 15 cm/sec, respectively. The suite consists of 16 site class D sites (stiff soil) and 6 site class C sites (very stiff soil), which matches the site class D of the designed CRSBFs well. For the time-history analysis, each of the 44 ground motions was scaled so that the spectral acceleration of each motion matches the DBE design spectrum at the fundamental period of the designed CRSBF. An example of the scaled response spectra of the 44 ground motions is shown in Figure 4.
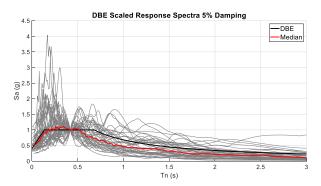
Figure 4. Ground motions scaled to DBE spectrum at fundamental period.

CONTROLLED ROCKING STEEL BRACED FRAME OPENSEES MODELLING

The CRSBFs were modelled using OpenSees [13] and time-history analyses of the 44 scaled ground motions were used to generate the floor displacement and acceleration responses. The schematic of the CRSBF OpenSees model is shown in Figure 5. All frame members (beams, columns and braces) were modelled using elastic beam-column elements. Rigid links were provided at brace connection joints to model the behaviour of the brace gusset plates. Column elements were modelled as continuous. The prestressing and friction energy dissipation devices were modelled using corotational truss elements. The prestressing element was modelled with an initial stress material to account for the designed prestress, as well as a multi-linear material to allow for yielding. The prestressing element was attached at the top of the frame and was anchored at the base to a tension only gap element to prevent it from developing any compression. The friction energy dissipation device was modelled with an elastic perfectly plastic material that has an essentially infinite initial stiffness. Horizontal and vertical gap elements were used at the base of each column and were modelled with compression rigid, elastic-no tension materials allowing each toe to act as a pin while the frame rocks in one direction, but freely allow uplift when the frame rocks in the other. Finally, a leaning column was included to account for the P-Delta moment effects caused by the gravity loads of the floor diaphragms acting at the frame displacement. The entire mass of the floor and roof diaphragms was lumped at the leaning column nodes, which were also constrained to displace laterally with the centre joints of the frame. A tangent stiffness and mass proportional Rayleigh damping model was used for the time-history analysis. An inherent damping ratio of 2% was applied to the first and second modes in order to calculate the Rayleigh damping coefficients. Full details of the model are provided by Steele and Wiebe [12].
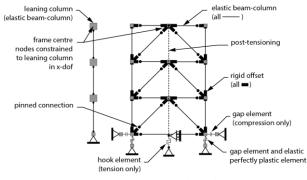

Figure 5. OpenSees model schematic

TIME-HISTORY ANALYSIS RESULTS AND DISCUSSION

Structural Performance

Table 1 shows the main structural performance results for the four CRSBF designs. The number of ground motions that led to column buckling and brace buckling, as well as the median peak drifts for the time-history analyses of each CRSBF, are also shown in Table 1. The median peak storey drift ratios of the four designs were between 1.35% and 1.47%. The small range of median peak drifts suggests that the performance of displacement-sensitive attached nonstructural components would be similar in all four CRSBFs, allowing for the performance of acceleration-sensitive components to be compared between the four designs from the perspective of equal displacement performance. No more than three ground motions caused a column to buckle in any of the four CRSBF designs. For the $\beta = 25\%$ CRSBFs, the design with $\eta = 20\%$ experienced brace buckling in one out of 44 ground motions, and the design with $\eta = 40\%$ experienced brace buckling in seven out of 44 ground motions. For the $\beta = 90\%$ CRSBF designs, brace buckling occurred in six ground motions for both the $\eta = 20\%$ and $\eta = 40\%$ designs.

5

Although the OpenSees model does not account for inelastic behaviour of the frame members, buckling occurred in less than 16% of the ground motions, which was deemed acceptable for comparing the nonstructural component performance between each of the CRSBFs. Since the fundamental rocking mode dominates the displacement response of the CRSBFs, each design follows a nearly uniform profile of storey drifts, as shown in the top-left of Figure 6, which presents the response of the CRSBF designed with $\beta = 25\%$ and $\eta = 20\%$. Uniform storey drifts are one advantage of CRSBFs with respect to displacement-sensitive nonstructural components, as the drifts tend not to concentrate at any one storey. The top-right and bottom-left graphs in Figure 6 show the distribution of brace and column peak axial loads for all 44 ground motions in comparison to the member buckling loads at each storey, confirming that for at least 84% of ground motions with all designs, the capacity design procedure was successful in avoiding any buckling or yielding in the frame. For this study, collapse was defined as any CRSBFs that exceeded a 10% storey drift. Collapse occurred in no more than three out of 44 ground motions for any of the designs.
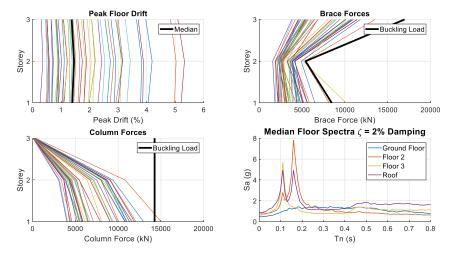

Figure 6. CRSBF time-history analysis results for design with $\beta = 25\%$ and $\eta = 20\%$

Attached Nonstructural Component Performance

Figure 7 compares the 2% damped median pseudo acceleration floor spectra at each floor level for the four designed CRSBFs. The amplification of the ground floor spectra throughout the height of the structure is significant, as the pseudo acceleration peaks exceed 5 g at all floors. Demands of similar magnitude were observed in the study by Pollino [16] on a three-storey CRSBF in Los Angeles, with the 5% damped floor spectra peaks ranging from about 3.5 g to 5.5 g in the CRSBF.

The median peak ground accelerations were between 0.47 g and 0.51 g, depending on the period at which the ground motions were scaled. The average of the peak floor accelerations (PFAs) of the CRSBFs was 0.75 g on the second floor, 0.53 g on the third floor and 0.78 g at the roof, and did not follow any apparent trend between the four designs. The largest difference among designs in the PFA at any floor was only 0.29 g, occurring on the third floor.
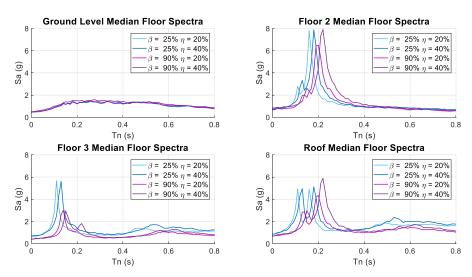

Figure 7. CRSBF median floor spectra with $\zeta = 2\%$

A comparison of the floor spectra between the four CRSBF designs does not reveal any major differences in floor spectra magnitude caused by altering the amount of energy dissipation or the prestress ratio; however, both of the designs with $\beta = 25\%$ have higher participation in the third mode relative to the designs with $\beta = 90\%$, leading to higher peaks in spectral accelerations near the third-mode periods (see Table 1) for all floors and designs. Besides this difference, the similar magnitudes and trends of the floor spectra suggest that the wide range of energy dissipation and prestressing chosen between the four designs has little effect on the floor acceleration responses, which are likely driven by the stiffness of the frame.

Although the peaks in pseudo acceleration are not dramatically different in magnitude for different designs, the peaks in the floor spectra do shift. This observation is likely caused by the difference in fundamental periods of each CRSBF, rather than the change in design parameters β and η. With reference to Table 1, the sequence of peaks in Figure 7 is consistent with the sequence of the natural periods of each CRSBF. Because of the stiff nature of attached nonstructural components, it could be advantageous to have a CRSBF that meets target drifts with the longest possible fundamental period, which might also push the peaks of the floor spectra outside the range of many stiff attached components. As a point of reference, ASCE 7-16 [9] defines attached components as rigid when they have a period of less than or equal to 0.06, and flexible when they have a period of greater than 0.06. An estimation of the longest periods in various flexible components is up to: 0.13 for mechanical equipment, 0.3 for electrical equipment cabinets and 0.1 or 0.2 for a wide range of other electrical nonstructural components [9].

In order to further investigate the effects of the rocking joint design parameters and CRSBF natural periods on the floor spectra, the four rocking joint designs were combined with the stiffest capacity designed frame (i.e. the design with $\beta = 25\%$ and $\eta = 20\%$), and the time-history analyses were repeated. Figure 8 shows that the floor spectra become much more similar when the same frame is used for all four designs, thus confirming that the initial stiffness of the CRSBF plays a larger role in determining the floor spectra compared to the rocking joint design parameters. Nevertheless, the designs with more energy dissipation ($\beta = 90\%$) do show a slight reduction in floor spectra magnitudes.
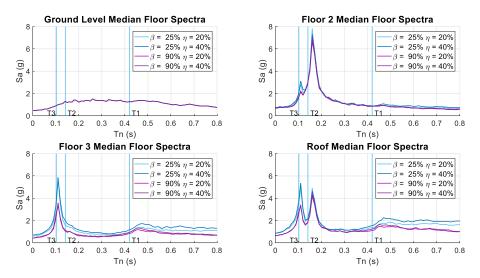

Figure 8. Floor spectra with different rocking joints but identical frames with $\zeta = 2\%$

The location of floor spectra peaks with respect to the periods of the CRSBF might also be of interest to a designer. Figure 8 shows the periods of the first three lateral modes of the $\beta = 25\%$, $\eta = 20\%$ design. The periods of the three other CRSBFs designed with identical frames have natural periods that are within 0.3% of the values plotted. The natural periods were taken from the fixed-base OpenSees CRSBF model, rather than the elastic model of the frame rocking about its toe used during the dynamic capacity design procedure. Each floor spectrum above the ground level shows two main peaks at natural periods of 0.11 s and 0.16 s. These peaks in the floor spectra for all designs seem to consistently occur not at, but just above, the natural periods of the third and second modes of the CRSBFs, which correspond to 0.102 s and 0.141 s as shown in Table 1. Instead, the peaks in floor spectra are located closer to the third and second modes of the elastic model of the frame rocking about its toe (used during the capacity design procedure), which were calculated as 0.111 s and 0.156 s, respectively. A similar observation can also be made for the floor spectra of the three other original CRSBF designs, shown in Figure 7.

CONCLUSIONS

Four three-storey CRSBFs were designed to meet a target seismic drift of 1.5% at the DBE level. The designs varied based on the amount of energy dissipation provided (β) and the prestress in the prestressed tendon (η). The designs reached similar median peak drifts, suggesting similar performance for displacement-sensitive nonstructural components, and the performance

of acceleration-sensitive nonstructural components was assessed using floor spectra. Although the floor spectra peaks were slightly reduced by increasing β for a given frame stiffness, the magnitudes and peak locations of the floor spectra were more affected by the stiffness of the CRSBF than by the rocking joint design parameters β and η. Therefore, the CRSBFs designed in this study show that when a similar performance in displacement-sensitive nonstructural components is achieved, the choice of hysteretic design parameters of the CRSBF rocking joint does not appear to play a major role in acceleration-sensitive component performance. Further studies would need to be performed to determine if these relationships are consistent for other CRSBF designs, as well as to compare the performance of nonstructural components in CRSBFs to that in more conventional systems that are already codified.

ACKNOWLEDGMENTS

REFERENCES

[1] Eatherton, M.R. and Hajjar, J.F. (2010). "Large-Scale Cyclic and Hybrid Simulation Testing and Development of a Controlled-Rocking Steel Building System with Replaceable Fuses". *Report NSEL-025*, Dept. of Civil and Env. Eng., University of Illinois at Urbana-Champaign, USA.

[2] Roke, D., Sause, R., Ricles, J.M. and Chancellor, N.B. (2010). "Damage-Free Seismic-Resistant Self-Centering Concentrically-Braced Frames". *ATLSS Report 10-09*, Lehigh University, USA.

[3] Ma, X., Krawinkler, H. and Deierlein, G. (2010). "Seismic Design and Behavior of Self-Centering Braced Frame with Controlled Rocking and Energy-Dissipating Fuses". *Report 174*, John A. Blume Earthquake Engineering Center, Stanford, CA, USA.

[4] Taghavi, S. and Miranda, E. (2003). "Response Assessment of Nonstructural Building Elements". *Report PEER 2003/05*, Pacific Earthquake Engineering Research Center, University of California, Berkeley.

[5] Wiebe, L., Christopoulos, C., Tremblay, R. and Leclerc, M. (2013). "Mechanisms to Limit Higher Mode Effects in a Controlled Rocking Steel Frame. 2: Large-Amplitude Shake Table Testing". *Earthquake Engineering & Structural Dynamics*, 42, 1069–1086.

[6] Wiebe, L. and Christopoulos, C. (2010). "Characterizing Acceleration Spikes Due to Stiffness Changes in Nonlinear Systems". *Earthquake Engineering & Structural Dynamics*, 39, 1653–1670.

[7] Dyanati, M., Huang, Q. and Roke, D. (2014). "Structural and Nonstructural Performance Evaluation of Self-Centering Concentrically Braced Frames Under Seismic Loading". *Proceedings of ASCE 2014 Structures Congress*, Boston, MA, USA.

[8] Pollino, M. (2014). "Seismic Design for Enhanced Building Performance Using Rocking Steel Braced Frames". *Engineering Structures*, 83, 129–139.

[9] American Society of Civil Engineers (ASCE), (2016). Minimum Design Loads for Buildings and Other Structures, ASCE/SEI Standard 7-16, American Society of Civil Engineers, Reston, VA, USA.

[10] Wiebe, L. and Christopoulos, C. (2015). "Performance-Based Seismic Design of Controlled Rocking Steel Braced Frames. I: Methodological Framework and Design of Base Rocking Joint". *Journal of Structural Engineering*, 141(9): 04014226.

[11] Zhang, C., Steele, T.C. and Wiebe, L. (2018). "Design-Level Estimation of Seismic Displacements for Self-Centering SDOF Systems on Stiff Soil". *Engineering Structures*, 177, 431–443.

[12] Steele, T.C. and Wiebe, L. (2016). "Dynamic and Equivalent Static Procedures for Capacity Design of Controlled Rocking Steel Braced Frames". *Earthquake Engineering & Structural Dynamics,* 45, 2349–2369.

[13] OpenSees. (2015) Open System for Earthquake Engineering Simulation v2.4.4 [Computer Software]

[14] Wiebe, L. and Christopoulos, C. (2015). "Performance-Based Seismic Design of Controlled Rocking Steel Braced Frames. II: Design of Capacity-Protected Elements". *Journal of Structural Engineering*, 141 (9): 04014227.

[15] Applied Technology Council. (2009). Quantification of Building Seismic Performance Factors, *FEMA Report P695,* Prepared for Federal Emergency Management Agency: Washington, DC, United States.

[16] Pollino, M. (2012). "Structural and Non-structural Seismic Demands on Controlled Rocking Steel Braced Frame Buildings". *Proceedings of ASCE 2012 Structures Congress*, Chicago, IL, USA.